5. Transport in fuel cell systems (Mench, ch. 5)

1. Ion transport in an electrolyte
2. Electron transport
3. Gas-phase mass transport
4. Single-phase flow in channels

(5. Multiphase mass transport in channels and porous media)

6. Heat generation and transport

1. Ion transport in fuel cell systems

-the rate of ion transport through the electrolyte $\propto$ current flow

n_j : molar rate of transfer of the ion through the electrolyte

z_j : charge number of the ion ($z = 1$ for H^+, $z = -2$ for O^{2-})

-transfer of ions through the electrolyte

(i) mass diffusion: a result of a concentration gradient

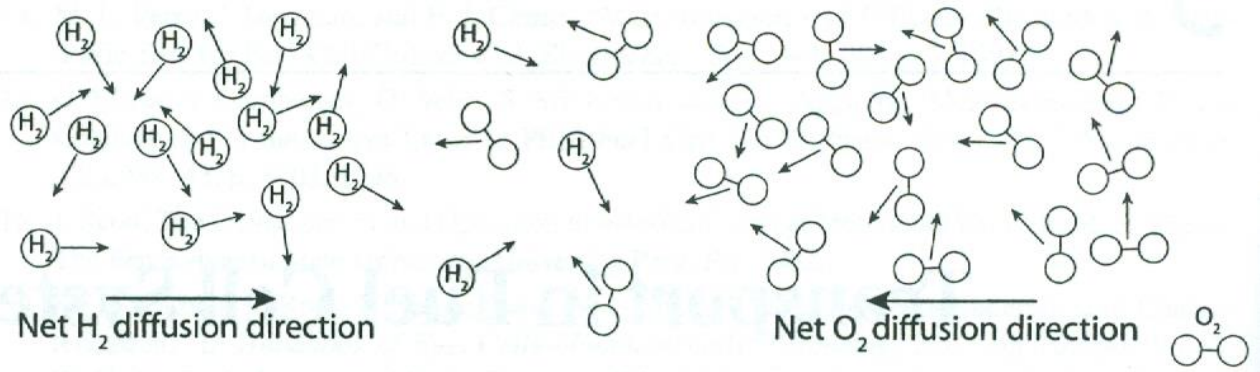

Figure 5.1 Diffusion mass transfer results from concentration gradient.

mass flow rate of the j ion in the x, y, z directions

→ three equations

(-) sign: mass transport in direction of decreasing conc of j

$D_{j,i}$: mass diffusivity coefficient of j in the I direction

∂처 $/\partial x_i$: concentration gradient of j in the I direction

(ii) Convection: a result of the net motion of the electrolyte (e.g., stirred liquid solutions)

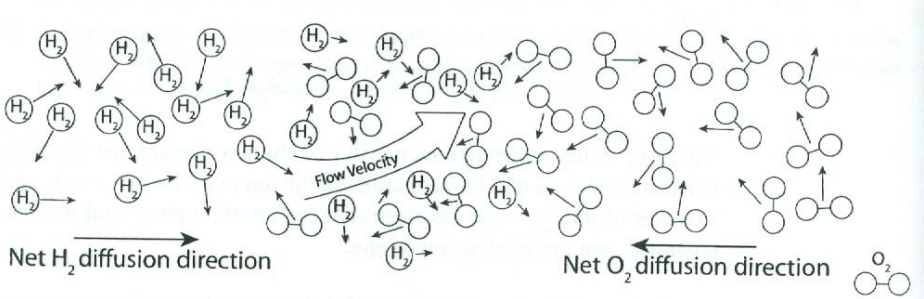

Figure 5.2 Convection mass transfer results from net motion of fluid.

v_i: solution velocity field vector

(iii) Migration: by an electrical potential difference

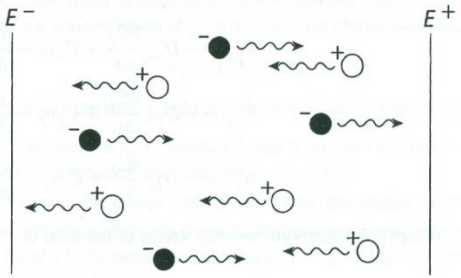

Figure 5.3 Migration mass transfer results from charged particles subjected to potential field gradient.

All modes together → Nernst-Plank equation governing ion transport

the following three equations in the x, y, and z directions:

$$\dot{n}''_{j,x} = -D_{j,x}\frac{\partial C_j}{\partial x} + C_j v_x - \frac{z_j F}{R_u T} D_{j,x} C_j \frac{\partial \phi}{\partial x} \tag{5.6}$$

$$\dot{n}''_{j,y} = -D_{j,y}\frac{\partial C_j}{\partial y} + C_j v_y - \frac{z_j F}{R_u T} D_{j,y} C_j \frac{\partial \phi}{\partial y} \tag{5.7}$$

$$\dot{n}''_{j,z} = -D_{j,z}\frac{\partial C_j}{\partial z} + C_j v_z - \frac{z_j F}{R_u T} D_{j,z} C_j \frac{\partial \phi}{\partial z} \tag{5.8}$$

where the electrolyte velocity vector of the fluid is

$$\mathbf{v} = v_x \mathbf{i} + v_y \mathbf{j} + v_z \mathbf{k} \tag{5.9}$$

From Eqs. (5.1) and (5.5), we can show in general that

$$i = \left(-D_{j,i}\frac{\partial C_j}{\partial x_i} + C_j v_i - \frac{z_j F}{R_u T} D_{j,i} C_j \frac{\partial \phi}{\partial x_i} \right) z_j F \tag{5.10}$$

The mobility u_j of ion j in the electrolyte is an important parameter related to the diffusion coefficient D_j through the Nernst–Einstein relation [1]:

$$u_j = \left| \frac{z_j F^2 D_j}{R_u T} \right| \tag{5.11}$$

→ mobility is a function of ionic charge, operating temp, pressure, ionic concentration, ion size.

-Despite the equation, mobility typically increase with T due to a decrease in the viscosity of electrolyte, which increase diffusivity

-Mobility of ions in solutions: $10^{-3} \sim 10^{-4}$ cm^2/Vs at 25° C

-Using mobility

In static electrolyte systems, $v_i = 0$

-At open-circuit conditions in a static electrolyte, the diffusion and migration transport will balance each other, so there is no net-current

-Liquid viscosity

$$\ln \frac{\mu}{\mu_o} = a + b\left(\frac{T_o}{T}\right) + c\left(\frac{T_o}{T}\right)^2 \qquad (5.13)$$

Values for the empirically derived constants can be found in various resources, and mixture relations can be used to estimate solution viscosities. For water, $a = -1.94$, $b = -4.80$, and $c = 6.75$ with $T_o = 273.16$ K and $\mu_o = 0.001792$ kg/(m · s).

- Conductivity

Conductivity A convenient relationship exists between the ionic conductivity (σ_j), mobility (u_j), and ion concentration (C_j) in a single ion carrier electrolyte [1]:

$$\sigma_j = F|z_j|u_j C_j \tag{5.14}$$

This expression provides physical insight into the ion conduction process in an electrolyte:

1. As the charge number z_j is increased, the total current carried per ion increases proportionally, increasing the effective conductivity.
2. As the mobility of the charge carriers increases, the conductivity increases.
3. As the concentration of charge carriers (participants in the ion exchange) increases, the ionic conductivity increases, although this trend does not hold for highly concentrated solutions.

Plugging in our expression for mobility, Eq. (5.11), we can glean a little more physical insight into the ion transport process.

$$\sigma_j = \frac{F^2}{R_u T} z_j^2 D_j C_j \tag{5.15}$$

From this expression, we can see that the conductivity of an electrolyte is strongly related to the diffusivity, ion concentration, and charge number. This relationship predicts a

(1) Solid polymer electrolytes

-ion mobility is a result of an electrolyte solution integrated into an inert polymer matrix

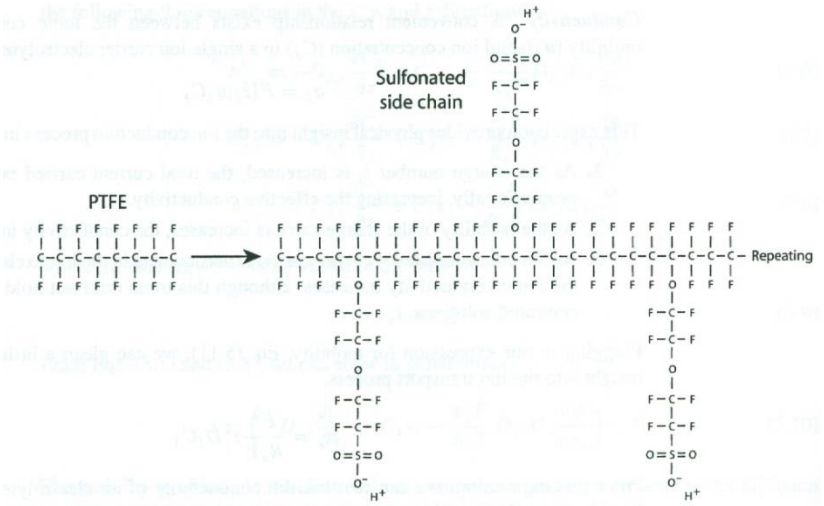

Figure 5.4 Schematic of sulfonated polytetrafluoroethylene (PTFE) structure used as ion-conducting electrolyte in PEFCs.

Most solid electrolytes: perfluorinated ionomers with a fixed side chain of sulfonic acid bounded covalently to the inert, but chemically stable, polymer polytetrafluoroethylene(PTFE) structure

→ two sub-structures:

(a) hydrophilic and ionically conductive phase that absorbs water

(b) hydrophobic and relatively inert polymer backbone which provide chemical stability and durability

e.g. Nafion: when hydrated, H_3O^+ - SO_3^- groups enable motion of H^+ ions

-two modes of transport

(a) Under low water content, proton transport is dominated by a vehicular mechanism or diffusion, where proton transport is direct, and by purely physical means

(b) With high hydration in the electrolyte, a proton hopping, a Grotthus mechanism is observed, with concomitantly higher effective proton conductivity. Protons "hop" from one H_3O^+ to another along a connected pathway in the ionomer structure

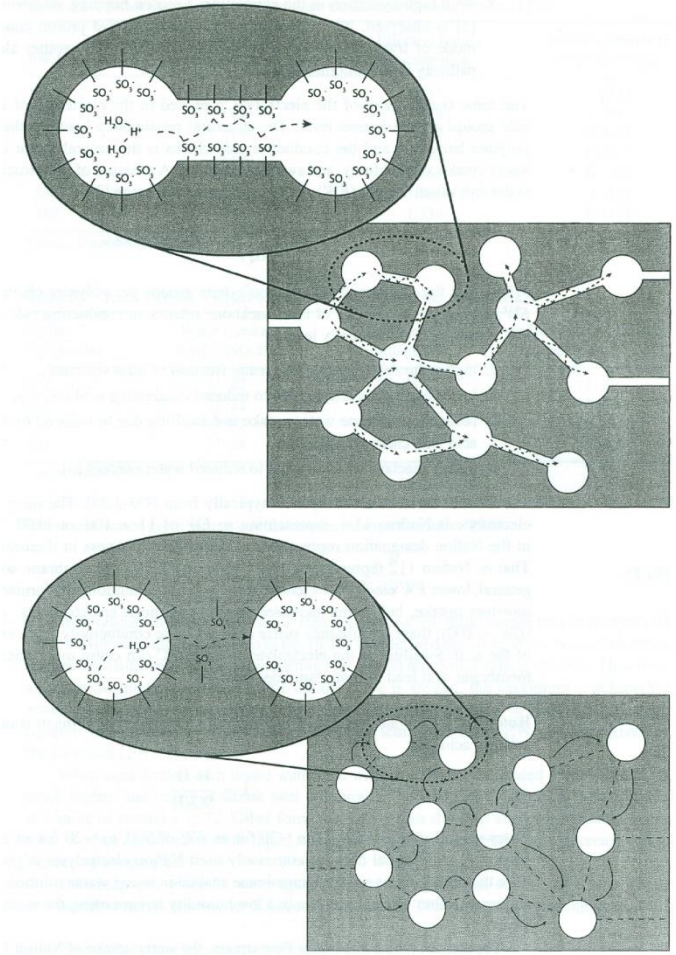

Figure 5.5 Schematic of connected sulfonated side chains which enable proton conduction through (*a*) Grotthuss and (*b*) vehicular mechanisms in wet and dry PEFC electrolyte membranes, respectively. (Adapted from Weber and Newman [5].)

-Ionic conductivity is related to the clustering of the sulfonic acid side chain groups and hydration level

-Equivalent weight of ionomeric membrane, EW(g/eq) = 100k + 446

k: # of tetrafluoroethylene groups per polymer chains

-EW↑ → inert backbone↑
-higher EW: (a) higher durability, (b) lower ionic conductivity, (c) reduced membrane water uptake and swelling, (d) higher reactant solubility due to reduced water content
-EW for FC electrolytes: typically 800~1200
-Nafion 11X: representing EW of 11 x 100 or 1100
X: dry electrolyte thickness in thousandths of an inch
112: 0.002″ (51μm) with 1100 EW
→ lower EW: better low-humidity performance due to higher moisture uptake

-Water uptake (λ): water molecules per sulfonic acid site

$$\lambda = H_2O / SO_3H$$

~30 for EW of 900, ~20 for EW of 1100
-For contact with a gas-phase flow stream, the water uptake of Nafion 1100EW at 30° C

$$\lambda = 0.043 + 17.18a - 39.85a^2 + 36.0a^3 \text{ for } 0 < a \leq 1$$

$$a = RH(\text{relative humidity}) = y_v P / P_{sat}(T)$$

Table 5.1 Water Uptake, Swelling, and Ionic Conductivity versus EW in a PEFC

EW (g/eq)	Water Uptake (wt %)	Effective Ionic Concentration	Ionic Conductivity at 23°C (S/cm)
1500	13.3	1.245	0.0123
1350	19.4	1.338	0.0253
1200	21.0	1.492	0.0636
1100	25.0	1.591	0.0902
980	27.1	1.764	0.1193
834	53.1	1.761	0.1152
785	79.1	1.539	0.0791

Source: Adapted from [8].

Table 5.2 Water Uptake, Weight Percent, and Swelling for Nafion Membranes

Nafion Designation	Water Uptake, λ (H_2O/SO_3H)	Water Weight Percentage (%)	Thickness Strain from Water Uptake, t_{wet}/t_{dry}
112	21–22	24–26	14–21
115	21–22	24–26	14–18
117	21–22	24–26	13–15
105	27–28	32–33	26–30

Source: Adapted from [9].

Example 5.1 Water Uptake in Nafion

Plot the expected water uptake in Nafion as a function of RH and include Schroeder's paradox uptake value of 22 at 80◦C and a water activity of one for liquid water.

-Nafion ionic conductivity:

strongly related to the hydration level,

temp effect → Nafion 1100EW over 25~90° C and full humidity range

$$\sigma_i \left(\frac{\mathrm{S}}{\mathrm{cm}}\right) = \exp\left[1268\left(\frac{1}{303} - \frac{1}{T}\right)\right](0.005193\lambda - 0.00326) \qquad (5.20)$$

$$\sigma_e \approx 0 \qquad (5.21)$$

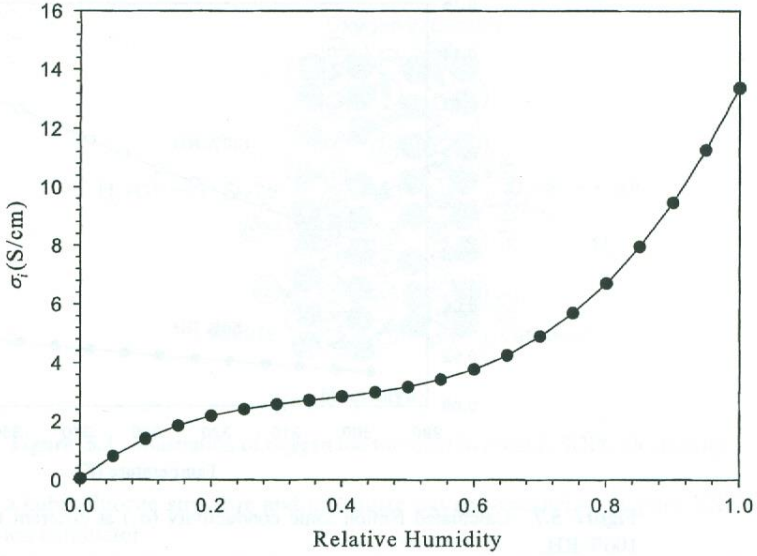

Figure 5.6 Calculated Nafion ionic conductivity (σ_i) at different RH values at 80°C.

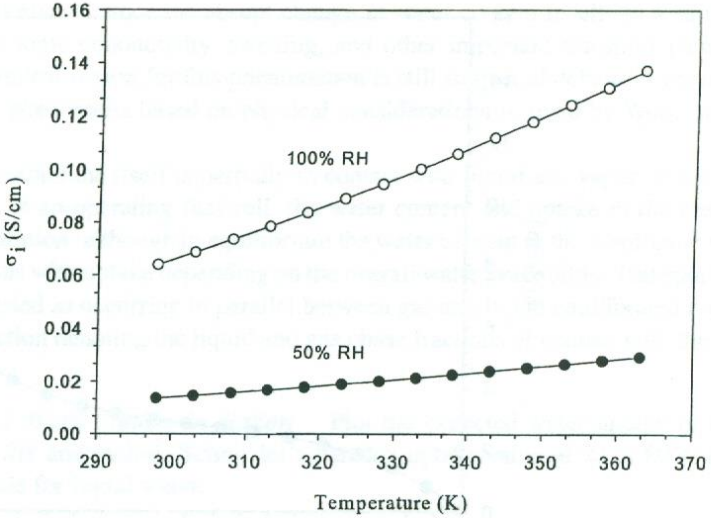

Figure 5.7 Calculated Nafion ionic conductivity (σ_i) at different temperature values at 50 and 100% RH.

RH>0.6: water weak bonding to sulfonic acid

→ unbound-like water

Example 5.2

Determine the ohmic drop through a Nafion 112 electrolyte in a 50% RH environment at 80◦C, 1A/cm^2.

(2) Ceramic electrolytes

-SOFC(solid oxide fuel cell): O^{2-} ions passed from cathode to anode via oxygen vacancies

→ ionic mobility : 2~3 orders lower than polymer or liquid

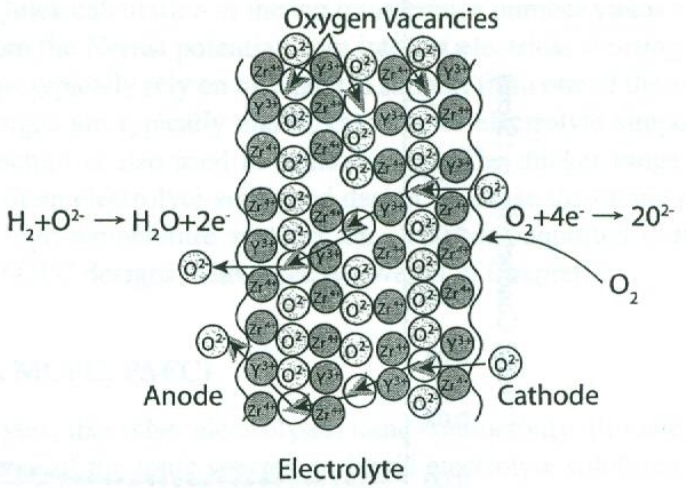

Figure 5.8 Illustration of oxygen ion transport in ceramic SOFC electrolytes.

e.g. YSZ (yttria(Y_2O_3) stabilized zirconia (ZrO_2) → high T is required for adequate oxygen ion conductivity

-YSZ: mixed (electronic and ionic) conductivity, but electrical conductivity is nearly negligible for typical operating conditions in the SOFC

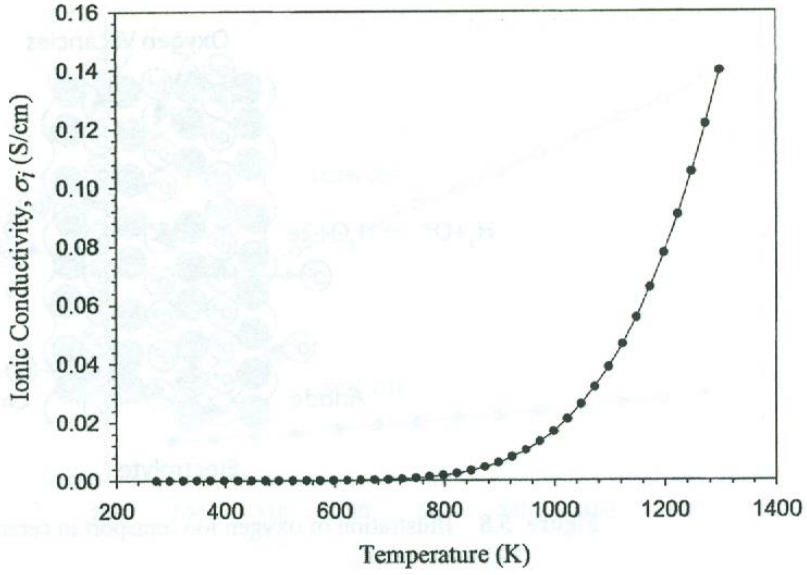

Figure 5.9 Ionic conductivity of $(ZrO_2)_{0.92}(Y_2O_3)_{0.08}$ as function of temperature.

Example 5.3 Ohmic Losses in SOFC as a Function of Electrolyte Thickness

Plot an ohmic-only polarization curve for a SOFC with $(ZrO_2)_{0.92}(Y_2O_3)_{0.08}$ electrolyte at 1000◦C for a 50-, 100-, and 300-µm-thick electrolyte and an OCV of 0.997V. That is, ignore kinetic and concentration polarization losses. Assume neat hydrogen and air at 1atm back pressure is used.

(3) Liquid electrolytes (AFC, MCFC, PAFC)

-AFC(alkaline FC), MCFC(molten carbonate FC), PAFC(phosphoric acid FC)

-ionic conductivity depends on the mobility and charge of the ionic species (solvated by strong dipoles of water)

-Charged particle in a potential vector field of strength $d\varphi_i/dx = \mathbf{E} \rightarrow$ a motive force $\mathbf{F} = z_j e\mathbf{E}$, e: 1.602 x 10^{-19} C, z: charge on the ion

-In the steady state, a spherical ion moving in a viscous field has a friction retarding force

$\mathbf{F} = 6\pi\nu r_j z_j v$, ν: viscosity(=η), r: ion radius, v: ion velocity

-maximum velocity of ion under electric field force

$$z_j e\frac{d\phi}{dx_i} = 6\pi\nu r_j \mathbf{V} \Rightarrow \mathbf{V} = \frac{z_j e(d\phi/dx_i)}{6\pi\nu r_j} \tag{5.25}$$

In addition to the relationship shown in Eq. (5.11), the ionic mobility u_j of an ion in an electrolyte in solution is really a measure of the maximum velocity of the ion for a given potential field:

$$u_j = \frac{V}{|d\phi/dx_i|} \tag{5.26}$$

-Ionic conductivity in liquid electrolyte is a function of the following

(a) Ionic concentration: optimal ion concentration (ion-ion interaction at high conc.) concentration↑ → σ↑

(b) Ionic mobility: related to viscosity, radius, ion charge number

(c) Temperature through viscosity

(d) Atomic radius: effective ionic radii (including solvating water)

(e) Ion charge: higher conc → higher σ. However, higher charge → water solvation↑ → increased effective radius → mobility↓

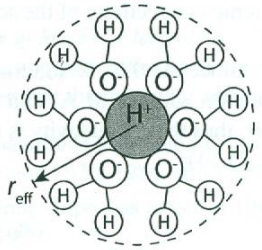

Figure 5.10 Illustration of effective ionic radius of solvated ion.

Table 5.3 Some Typical Electrolyte Conductivities Under Operation for Various Liquid Electrolyte Fuel Cells

Type of Fuel Cell	Electrolyte	Temperature (°C)	Ionic Conductivity σ (S/cm)
Alkaline (AFC)	KOH in 30–50% water	60–80	~0.4
Phosphoric acid (PAFC)	Concentrated H_3PO_4	200	~0.6
Molten Carbonate (MCFC)	Li_2CO_3 and K_2CO_3	650	~0.3

Source: From [16].

2. Electron transport

-mostly ignored in fuel cell due to littile contribution to the overall FC polarization

-this may not be true including (a) a poorly assembled cell, (b) an aged cell with some oxidation on current collector contacts

-electrical conductivity

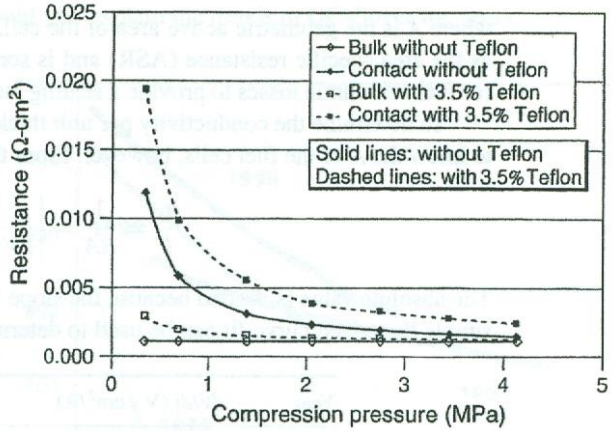

Figure 5.11 Through plane electrical resistance as function of compression pressure for common carbon fiber paper used as gas diffusion layer in PEFCs. The gas diffusion layers typically have some fraction of PTFE added to promote liquid water removal, which increases electrical bulk and contact resistance. (Reproduced from Ref. [18].)

3. Gas-phase mass transport

(1) General Diffusion

-average diffusion coefficient is a function of

(a) Other species present. Other molecules will collide with the diffusing species and different the net rate of motion

(b) Number of molecules, which corresponds to pressure. Number of molecules↑ → collisions↑ → average diffusion coefficient↓

(c) Velocity of the molecules, which is proportional to temperature

(d) Size and mass of molecules

-diffusion is a spontaneous process that is a result of 2^{nd} law of thermodynamics → maximum velocity

Fick's law of diffusion

For 1-D,

D_j: 0.1 cm^2/s (gases), 10^{-5} cm^2/s (liquids), 10^{-10} cm^2/s (solid-state, but strong function of temp → 15 orders of magnitude)

-diffusion of gases into solid polymers: ~10^{-8} cm^2/s (liquids)

Table 5.4 Some Experimental Gas-Phase Diffusion Coefficients at 1 atm

Gasl Pair	Temperature (K)	D (cm^2/s)
Air–O_2	273	0.176
Air–H_2O	298	0.260
Air–He	282	0.658
O_2–H_2O	308	0.282
N_2–O_2	293	0.220
O_2–He	317	0.822
Air–H_2	282	0.710
H_2–H_2O	307	0.915
H_2–He	317	1.706
H_2–CO_2	298	0.646
CO–H_2	296	0.743

Source: From [19].

Table 5.5 Diffusion Coefficients in Water at 298 K and Infinite Dilution

Gas into Water	Chemical Formula	D (cm^2/s)
Air	$(N_2)_{0.79}(O_2)_{0.21}$	2.00×10^{-5}
Carbon monoxide	CO	2.03×10^{-5}
Carbon dioxide	CO_2	1.92×10^{-5}
Hydrogen	H_2	4.50×10^{-5}
Methane	CH_4	1.49×10^{-5}
Oxygen	O_2	2.10×10^{-5}
Methanol	CH_3OH	0.84×10^{-5}
Ethanol	C_2H_6O	0.84×10^{-5}
Formic acid	CH_2O_2	1.50×10^{-5}
1-Propanol	$CH_3CH_2CH_2OH$	0.87×10^{-5}

Source: From [19].

Table 5.6 Some Representative Solid-Phase Diffusion Coefficients

System	Temperature (K)	D (cm^2/s)
Hydrogen in SiO_2	293	4.0×10^{-10}
Cerium in tungsten	2000	95×10^{-11}
Hydrogen in nickel	358	1.16×10^{-8}
Sliver in aluminum	323	1.2×10^{-9}
Aluminum in copper	293	1.3×10^{-30}

Source: From [19].

-diffusion coefficient in mixture
-Transient diffusion → Fick's 2nd law

-characteristic time of diffusion, τ_d (time for diffusion to reach a given distance δ)

- **Calculation of binary gas-phase diffusion coefficients**

-using molecular dynamic theory

-for fuel cell with gas-phase reactants, effective binary (two-species) diffusion coefficient from kinetic theory

Table 5.7 Critical Temperature and Pressure Data for Fuel Cell Gases

Gas	Formula	T_c (K)	P_c (atm)
Water	H_2O	647.3	218.0
Hydrogen	H_2	33.2	12.8
Oxygen	O_2	154	49.8
Nitrogen	N_2	126	33.5
Air	Mix	133	37.2
Carbon dioxide	CO_2	304	72.9
Carbon monoxide	CO	133	34.5
Methanol	CH_3OH	513	78.5

Source: From [20].

-for greater accuracy for hydrogen → using molecular volumes (V)

Table 5.8 Diffusion Volumes for Eq. (5.34)

Gas	Formula	$\sum V_{ij}$
Water vapor	H_2O	12.7
Hydrogen	H_2	7.07
Oxygen	O_2	16.6
Nitrogen	N_2	17.9
Air	Mix	20.1
Carbon dioxide	CO_2	26.9
Carbon monoxide	CO	18.9

Source: From [19].

Example 5.6 Characteristic Times for Gas-, Liquid-, and Solid-State Diffusion

Estimate typical characteristic times for a gas into gas, a gas into a liquid, a gas into a solid, and a gas into a polymer to diffuse a distance of 1 mm.

- **Multicomponent diffusion approaches**

-mixed species (more than two species)

(a) Mixture property approach. e.g. N_2, O_2, H_2O in cathode.
determine mole fraction of the constitutes using saturation pressure,
evaluate diffusion coefficient,
evaluate the mixture diffusivity using molar averaging

(b) Ignore inert species approach → simply ignore inert species

(c) Stefan-Maxwell approach
Stefan-Maxwell equation for multicomponent diffusion flux
(x-direction)

$$\frac{dy_i}{dx} = \frac{1}{C} \sum_{j \neq i} \frac{y_i n_j - y_j n_i}{D_{ij}} \tag{5.36}$$

where C is the total molar concentration of the gas mixture and the y_i's are the mole fractions, which can be determined by the pressure and temperature based on the ideal gas law,

$$C = \frac{P}{R_u T} \tag{5.37}$$

The n terms are the molar flux of the components in the x direction. The effective binary diffusion coefficient of the various gas species combinations, D_{ij}, is calculated under specified temperature and pressure according to one of the methods already described. As an example, consider a mixture of oxygen, water vapor, and nitrogen. From Eq. (5.36), we get following equations for the gradients for oxygen, nitrogen, and water vapor mole fractions in the cathode:

$$\frac{dy_{O_2}}{dx} = \frac{R_u T}{P} \left(\frac{y_{O_2} n_{H_2O} - y_{H_2O} n_{O_2}}{D_{O_2-H_2O}} + \frac{y_{O_2} n_{N_2} - y_{N_2} n_{O_2}}{D_{O_2-N_2}} \right) \tag{5.38}$$

$$\frac{dy_{N_2}}{dx} = \frac{R_u T}{P} \left(\frac{y_{N_2} n_{H_2O} - y_{H_2O} n_{N_2}}{D_{N_2-H_2O}} + \frac{y_{N_2} n_{O_2} - y_{N_2} n_{O_2}}{D_{N_2-O_2}} \right) \tag{5.39}$$

$$\frac{dy_{H_2O}}{dx} = \frac{R_u T}{P} \left(\frac{y_{H_2O} n_{N_2} - y_{N_2} n_{H_2O}}{D_{H_2O-N_2}} + \frac{y_{H_2O} n_{O_2} - y_{O_2} n_{H_2O}}{D_{H_2O-O_2}} \right) \tag{5.40}$$

Example 5.7 Estimation of Diffusivity of Hydrogen and Oxygen in Water Vapor

Estimate the diffusivity of hydrogen in water vapor and oxygen in water vapor at 1 atm and 307 K and compare with experimental data in Table 5.4.

(2) Gas-phase flow in porous media

-gas with electrodes or gas diffusion layer in PEFC → porous nature inhibits the diffusion rate by

(a) porosity: zero porosity (gas diffusivity zero), one porosity (bulk diffusivity)

(b) Tortuosity (구불구불한 굽이): effective average path length through the porous media compared to direct linear path → more tortuous the path → the longer the effective path length → greater reduction in the effective diffusivity

-the effective diffusivity for gas-phase flow in porous media

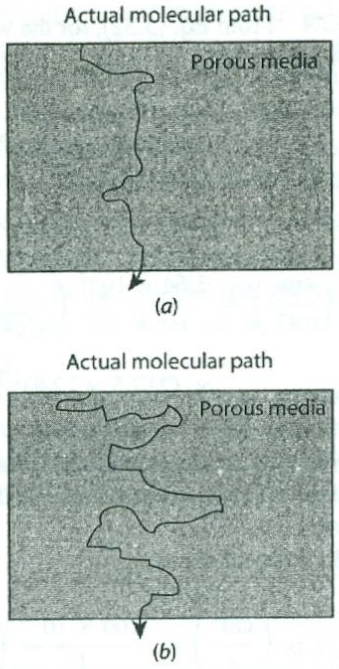

Figure 5.12 Illustration of porous media with (*a*) low and (*b*) high tortuosity.

Physically, the porosity correction is to adjust for the longer effective path length through the porous media. Using another approach, Salem and Chilingarian estimated tortuosity to be related to porosity for high-porosity material ($\phi = 0.62$–0.88) [24], which is appropriate for fuel cell media:

$$\tau = -2.1472 + 5.2438\phi \tag{5.43}$$

This relationship yields a value of $\tau \sim 1.5\phi$ for a typical PEFC diffusion layer ($\phi = 0.8$), or

$$D_{\text{eff}} = \frac{D}{1.5} \tag{5.44}$$

Comparing Eq. (5.44) to (5.42), there is not much difference between the result of using either approximation at high porosities typical of fuel cell media, especially given the inherent uncertainty of many other parameters involved.

- **Gas-phase limiting current density and diffusion resistance**

$$\underbrace{\frac{i_l A}{nF}}_{\text{Consumption}} = \underbrace{-D_j A \frac{dC_j}{dx}}_{\text{Diffusion transport}} + \underbrace{C_j A v_x}_{\text{Advective transport}} \tag{5.45}$$

where i_l is the mass transfer limiting current density. In some fuel cell designs, flow is intentionally forced to the surface by convection, which is the reason for the inclusion of the advective transport in Eq. (5.45). Additionally, the suction of reactant to the surface will naturally cause some bulk motion and convection near the electrode. However, this blowing/suction effect is typically small relative to the diffusion.

The diffusion rate is limited by flow through the porous media diffusion layer (PEFC and AFC) and electrode. If we assume one-dimensional flux to the electrode surface in the x direction with no bulk flow velocity (see Figure 5.13), we can write this as

$$i_l = -nFD_{\text{eff}} \frac{C_\infty - C_s}{\delta} = -nFD_{\text{eff}} \frac{C_\infty}{\delta} = -nFD_{\text{eff}} \frac{y_i P / R_u T}{\delta} \tag{5.46}$$

($C_s = 0$ at i_l)

where C_s, the surface concentration, is reduced to zero at the limiting condition and C_∞ is the concentration of the reactant at the boundary with the flow channel and is calculated with the ideal gas law. Here, δ is the distance to the electrode surface from the flow channel boundary. For high-temperature fuel cells, the diffusivity is usually high enough that the diffusion limiting current is not a factor. For the PEFC and AFC, the diffusion coefficient through the diffusion media is typically modified by the Bruggeman relationship to account

for the porosity:

$$i_l = -nFD_{\text{eff}}\frac{C_\infty}{\delta} = -nFD\phi^{1.5}\frac{y_i P/R_u T}{\delta} \tag{5.47}$$

This approach can easily be extended from just the diffusion media to include the catalyst layer as well. If we assume that the average reaction location is about midway through the catalyst layer of thickness γ, then we can write

$$i_l = -\,nFD_{\text{eff,DM}}\frac{C_\infty - C_{\text{DM}^+}}{\delta} = -\,nFD_{\text{eff,CL}}\frac{C_{\text{DM}^+} - C_s}{\gamma/2} \qquad C_s = 0 \tag{5.48}$$

where C_{DM^+} is the concentration of the reacting species at the diffusion media and catalyst layer interface. Solving for C_{DM^+} and plugging back in, we can show that

$$i_l = -nFD_{\text{eff,DM}}\frac{C_\infty - i_l\gamma/(2nFD_{\text{eff,CL}})}{\delta} = \frac{nFD_{\text{eff,DM}}}{\delta}\left(\frac{y_i P}{R_u T} - \frac{i_l\gamma}{2nFD_{\text{eff,CL}}}\right) \tag{5.49}$$

If the porosities in the catalyst layer and diffusion media are the same so that the effective diffusivities in the diffusion media and catalyst layer are identical, we can show that

$$i_l = \frac{nFD_{\text{eff}}\,(y_i P/R_u T)}{\delta + \gamma/2} \tag{5.50}$$

which is a result we could have expected. If the porosities are not the same (as is often the case), then Eq. (5.48) can be solved for the limiting current as

$$i_l = \frac{nFD_{\text{eff,DM}}(y_i P/R_u T)}{\delta + \gamma D_{\text{eff,DM}}/(2D_{\text{eff,CL}})} = \frac{nFD\phi_{\text{DM}}^{1.5}(y_i P/R_u T)}{\delta + (\gamma/2)(\phi_{\text{DM}}^{1.5}/\phi_{\text{CL}}^{1.5})} \tag{5.51}$$

Example 5.8 Calculation of Gas-Phase Transport Limited Current Density through Diffusion Media

Calculate the oxygen and hydrogen gas-phase transport limiting current density in a hydrogen PEFC for the anode and cathode sides at 80◦C, 2 atm pressure operation with fully humidified gas streams and high stoichiometry. Assume the anode

5.3 Gas-Phase Mass Transport 221

and cathode diffusion layers are 300 μm thick with 70% porosity. Ignore the catalyst layer restriction in this problem.

(3) Knudsen(크누센) diffusion

-for diffusion through very small pores → Knudsen diffusion dominant at small pore sizes where wall interactions become significant → adding "wall viscosity", which acts to retard motion

-key parameter in Knudsen diffusion is the average path length of the molecules between collisions → path length ≈ pore diameter → wall interaction (Knudsen diffusion) is important

-mean free path length (for gas)

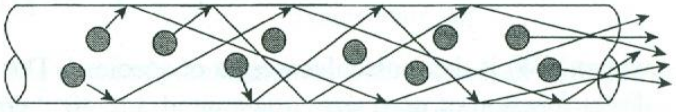

Figure 5.15 Flow in a very small channel. The molecular interactions with the channel wall are no longer negligible compared to the collisions with other molecules.

Table 5.9 Collision Diameters σ_{ii} for Various Fuel Cell Species From

Species	Formula	σ_{ii} (Å)
Carbon dioxide	CO_2	3.941
Carbon monoxide	CO	3.690
Hydrogen	H_2	2.827
Oxygen	O_2	3.467
Nitrogen	N_2	3.798
Hydrogen peroxide	H_2O_2	4.196
Hydrogen sulfide	H_2S	3.623
Methanol	CH_3OH	3.626
Water	H_2O	2.641
Dimethyl ether	CH_3OCH_3	4.307
Air	Mix	3.711

Source: From [19].

$(1.3807 \times 10^{-23}$ J/K). For example, for oxygen at 1 atm pressure and 1000 °C,

$$l = \frac{(1.3807 \times 10^{-23}\ \text{N} \cdot \text{m/K})\,(1273\ \text{K})}{\sqrt{2}\pi\,(3.467 \times 10^{-10}\ \text{m})^2\,(101{,}325\ \text{N/m}^2)} = 0.325\ \mu\text{m}$$

For hydrogen, we can solve for a path length of 0.489 μm under the same conditions In order to determine if Knudsen diffusion is significant, the Knudsen number (Kn) mus be calculated according to the following criteria:

$$\text{Kn} = \frac{l}{d} = \frac{k_B T}{\sqrt{2}\pi\sigma_{ii}^2 P d} \tag{5.53}$$

- When Kn > 10, Knudsen flow dominates.
- When Kn < 0.01, bulk diffusion flow dominates.
- For 0.01 < Kn < 10, both Knudsen and bulk diffusion are important and a combi nation flow exists.

For Knudsen flow, the effective diffusion coefficient can be determined from the kineti theory of rigid spheres [19]:

$$D_{\text{Kn}}\left(\frac{\text{cm}^2}{\text{s}}\right) = \frac{d}{3}\left[\frac{2k_B T}{m_i}\right]^{1/2} \tag{5.54}$$

where m_i is the molecular mass of species i. Alternate theory yields a larger value [15]:

$$D_{\text{Kn}}\left(\frac{\text{cm}^2}{\text{s}}\right) = \frac{4850 d\sqrt{T}}{\text{MW}_i} \tag{5.55}$$

where MW_i is the molecular weight of species i. The magnitude of Knudsen diffusion is direct function of pore size. It is around 3×10^{-3} cm^2/s for a 50-nm pore with hydroge diffusion at 353 K. As the molecular weight increases, Knudsen diffusivity decreases, an as pore diameter increases, diffusivity increases (less collisions to interfere with motion), t

the limit of transition to bulk diffusion. Also notice there is no pressure or multicomponent factor in Knudsen diffusion. This is because in the Knudsen limit intermolecular collisions are rare. Also notice bulk diffusion varies with $T^{1.5}$, where Knudsen diffusivity varies with $T^{0.5}$. Knudsen diffusion flux is modeled with the Fickian equation, with a modified Knudsen diffusion coefficient replacing the binary diffusion coefficient:

$$\dot{n}_j = -D_{\mathrm{Kn}} A \frac{dC_j}{dx} \tag{5.56}$$

Also note that the model assumes a straight pore path. As in bulk media, any tortuosity will increase the real path length, and this must be added to the result as in Eq. (5.41). In the context of the length scales involved with Knudsen diffusion, however, it is unlikely significant error will result without the use of a tortuosity correction.

Example 5.9 Knudsen Flow Estimate the pore diameters where Knudsen flow will be important as a function of temperature from 273 to 1000°C for oxygen and hydrogen at 1 atm.

SOLUTION We can easily solve for the mean molecular path length:

$$l = \frac{k_B T}{\sqrt{2}\pi \sigma_{ii}^2 P}$$

From this we can plot the regions where the ratio of l/d falls within the three flow regimes.

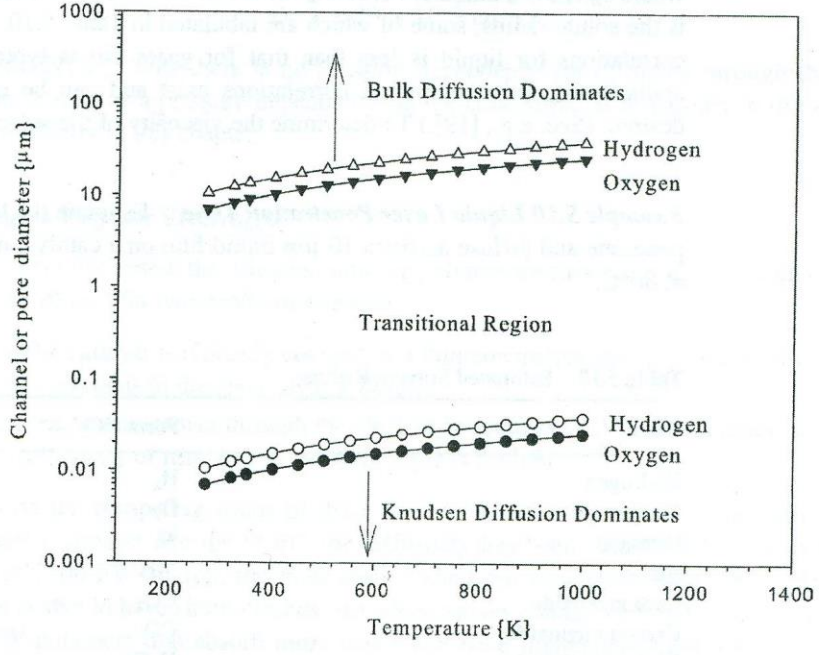

(4) Liquid-phase diffusion

-Table 5.4 and 5.5 → diffusion coefficient of gas in liquid to fall 10^{-5} cm^2/s range → in fuel cell, gas diffusion (i) in liquids occurs between the gas phase and liquid electrolyte, (ii) flooded condition in PEFC, (iii) liquid fuel in DMFC(direct methanol fuel cell)

-diffusion in liquids is so slow relative to gases → Stokes-Einstein equation used to establish liquid diffusion coefficient

Table 5.10 Estimated Solvent Radius

Gas	Formula	R_o (Å)
Hydrogen	H_2	1.414
Oxygen	O_2	1.734
Nitrogen	N_2	1.899
Air	Mix	1.856
Carbon dioxide	CO_2	1.971
Carbon monoxide	CO	1.845
Hydrogen peroxide	H_2O_2	2.098
Ethanol	C_2H_5OH	2.265
Methanol	CH_3OH	1.813

Source: Adapted from data in [19].

Example 5.10 Liquid Layer Penetration Time

Estimate the time required for oxygen to penetrate and diffuse across a 10-μm liquid film on a catalyst in a partially flooded PEFC at 80◦C.

(5) Diffusion through a polymer electrolyte

-why important in PEFC?

(i) The catalyst is typically covered in a thin electrolyte layer, so that high diffusivity of reactants in the electrolyte is desired

(ii) Reactant crossover through the electrolyte reduces open-circuit voltage and efficiency, so that low diffusivity of reactants in the electrolyte is desired

-low EW polymers that absorb more water will have higher gas-phase species diffusion coefficient than higher EW electrolytes

-diffusivity of water vapor into PEFC nafion electrolyte is function of the water uptake

the water uptake increases dramatically, and transport properties approach that of a dilute electrolyte solution.

The diffusivity of water vapor into PEFC electrolyte Nafion is a function of the material's water uptake, since the vapor must diffuse through the entire media. There is significant discrepancy between various authors on the measured values of the water diffusivity coefficient, since it is a difficult parameter to accurately measure, and the membrane itself swells with water uptake. The diffusion coefficient of water in 1100-EW Nafion PFSA polymer with $\lambda > 4$ has been correlated as [12]:

$$D_w\left(\frac{\text{cm}^2}{\text{s}}\right) = 10^{-6}\exp\left[2416\left(\frac{1}{303}-\frac{1}{T}\right)\right](2.563 - 0.33\lambda + 0.0264\lambda^2 - 0.000671\lambda^3) \tag{5.58}$$

where λ is given in Eq. (5.18). The diffusion coefficient of water in Nafion has been studied by many authors, and a surprising degree of difference between results exists, Eq. (5.58) is commonly used in modely however, and is considered a reasonable correlation. Oxygen diffusivity into 1100-EW Nafion has been given empirically as [26]:

$$D_{O_2-\text{Nafion}}\left(\frac{\text{cm}^2}{\text{s}}\right) = 2.88\times 10^{-6}\exp\left[2933\left(\frac{1}{313}-\frac{1}{T}\right)\right] \tag{5.59}$$

For 1200-EW polymer [27]:

$$D_{O_2-\text{Nafion}}\left(\frac{\text{cm}^2}{\text{s}}\right) = 3.1\times 10^{-3}\exp\left(-\frac{2768}{T}\right) \tag{5.60}$$

Both approaches yield the same order of magnitude in results. Hydrogen diffusivity into Nafion 1100-EW as a function of temperature (in Kelvin) for a fully moist Nafion 1100-EW polymer has been correlated as [28]

$$D_{H_2-\text{Nafion}}\left(\frac{\text{cm}^2}{\text{s}}\right) = 4.1\times 10^{-3}\exp\left(\frac{-2602}{T}\right) \tag{5.61}$$

It should be cautioned that the availability of precise transport coefficients is incomplete in the literature. There are significant differences between research results for much of these data, and complete details under a full range of temperature and humidity, and for all materials are not yet available. Nevertheless, the values presented here serve as a reasonable approximation to the diffusion coefficients for calculation purposes.

(7) Surface diffusion

-gas molecules absorb onto a solid surface (physically or chemically)
→ physical adsorption (highly mobile), chemisorption (not directly mobile, but move via a hopping mechanism)
-gas across the surface

(8) Diffusion summary

Table 5.12 Summary of Orders of Magnitude of Diffusion Coefficients for Various Modes of Transport

Mode of Diffusion	Order (cm^2/s)
Bulk gas in gas	$O(0.1)$
Dissolved gas in liquid	$O(10^{-5})$
Gas into liquid	$O(10^{-4})$
Knudsen	$O(10^{-3}–0)\, f$(pore size)
O_2/H_2 in Nafion	$O(10^{-6})$ at 353 K
Surface diffusion	$O(10^{-5}–10^{-7})$

4. Single-phase flow in channels

(1) Pressure drop

(i) Frictional loss

(ii) Consumption of reactant

(iii) Production of species

(iv) Two-phase flow or blockage

(i) **Frictional losses**: the ratio of momentum to viscous loss = Reynolds number Re

$$Re = \rho V d_h / \mu,$$

V: velocity, ρ: fluid density, μ(or η): fluid viscosity

d_h: hydraulic diameter ($=4A_x/P_w$),

A_x: cross-sectional area of flow

P_w: length of the perimeter w

For round channels (radius r)

$d_h = 4\pi r^2/2\pi r = 2r$

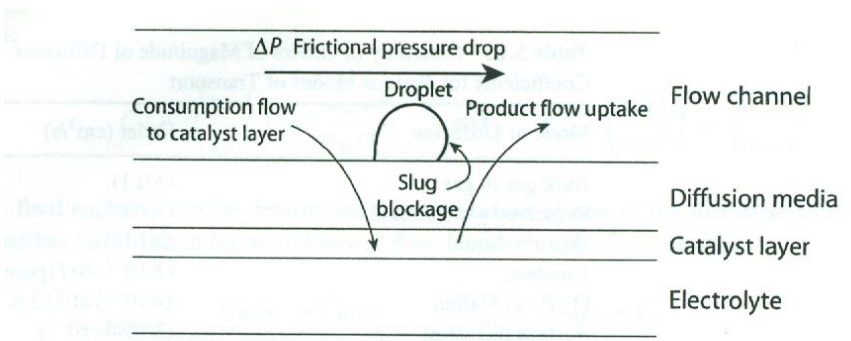

Figure 5.17 Schematic of pressure drop and mass exchange in the flow channel of fuel cell.

For rectangular channels (width w, height h)

$d_h = 4wh/(2w + 2h) = 2wh/(w + h)$

-For Re < 3000 in an internal channel → the flow laminar

(uniform streamlines & locally steady flow)

Re > 3000, turbulent flow

-Fuel cells: highly laminar

-the cause of the pressure drop for internal flow is the viscous interaction with the wall

Shear force at the wall for a Newtonian (laminar) fluid is proportional to the fluid strain and is related to fluid viscosity

$F_{wall} = \tau A = A\mu(du/dy)$

A: surface area of contact between the fluid and the wall

du/dy: slope of the change in velocity with distance from the wall

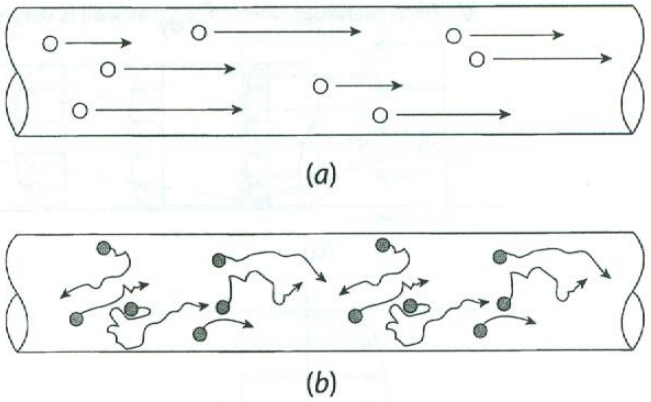

Figure 5.18 Illustration of individual particle flow trajectories in (*a*) laminar and (*b*) turbulent flow.

-To overcome shear force imposed by the channel walls and viscous walls → the flow experience pressure drop along the channel

$F_{wall} \uparrow \rightarrow \Delta P \uparrow$

-In open-filed flow

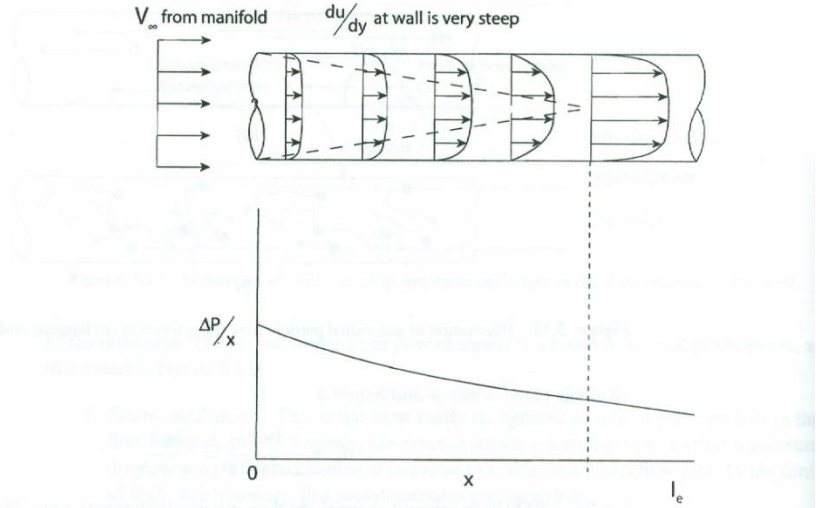

Figure 5.19 Developing flow profile in a channel. The shear forces that accumulate along the wall result in a pressure drop along the channel that must be provided for by the reactant flow system.

Turbulent → steeper du/dy

→ higher ΔP (pressure drop)

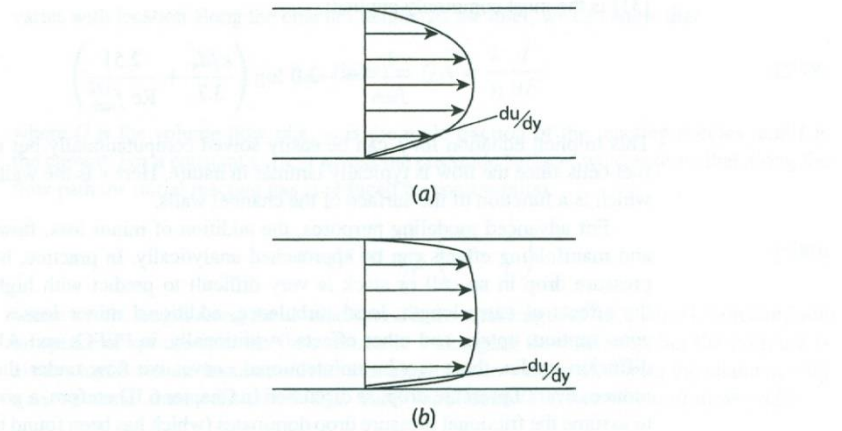

Figure 5.20 Laminar and turbulent profile boundaries: (*a*) fully developed laminar profile; (*b*) fully developed turbulent profile. Notice the turbulent du/dy profile is much steeper, leading to a higher pressure drop per unit length via Eq. (5.71).

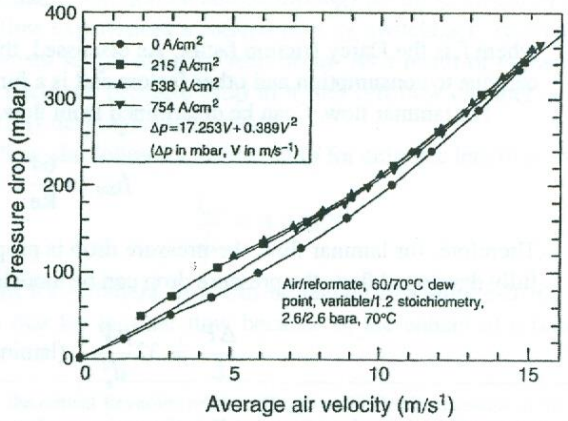

Figure 5.21 Measured and correlated pressure drop in a Ballard fuel cell as a function of velocity. (From Ref. [32] with permission.)

6. Heat generation and transport

(1) Heat generation

-In fuel cell, still considerable heat generation

high T SOFC → heat dissipation is not major issue

-For low T PEFC, heat generation is challenging

(i) In combustion engine, ~80% waste heat is removed by exhaust gas flow. In PEFC, waste heat is removed by coolant → additional burdens on the system

(ii) Heat transport rate ∞ temp difference between heat source to the ambient → lower heat rejection rate in low T fuel cell

-heat generation flux in a fuel cell to be related to the current and the departure of cell voltage from the thermal voltage

concentration polarizations. This heat generation includes the *reversible heat generated* by the entropy change, which is the difference in the thermal and Nernst voltages:

$$q''_{\text{heat,rev}}(\text{W/cm}^2) = i(E_{\text{th}} - E^\circ) = i\left(-\frac{\Delta H}{nF} - \frac{\Delta G}{nF}\right) = -i\frac{T\,\Delta S}{nF} \tag{5.108}$$

This entropy-generated heat is known as Peltier heating. The *irreversible heat generated* by activation, ohmic, and concentration polarizations is

$$q''_{\text{heat,irr}}(\text{W/cm}^2) = i(E^\circ - E_{\text{cell}}) = i(\eta_{a,a} + |\eta_{a,c}| + \eta_{m,a} + |\eta_{m,c}| + \eta_R + \eta_x) \tag{5.109}$$

where the various polarizations are defined in Chapter 4. The total heat generated by reaction polarizations is the sum of the reversible and irreversible components:

$$q''_{\text{total}}(\text{W/cm}^2) = -i\frac{T\,\Delta S}{nF} + i(\eta_{a,a} + |\eta_{a,c}| + \eta_{m,a} + |\eta_{m,c}| + \eta_R + \eta_x) \tag{5.110}$$

As current density increases (corresponding also to reduced cell voltage), the thermal energy dissipation flux will increase. The first term on the right-hand side of Eq. (5.110) represents Peltier heating. The second term on the right-hand side represents the sum of the activation (kinetic), concentration, ohmic, and crossover contributions to the heat generation.

(2) Single-phase heat transport

- **Conduction**: heat transfer resulting from intermolecular collisions → Fourier's law of heat conduction (analogue to Fick's law of mass diffusion)

Table 5.14 Measured Thermal Conductivity of Polymer Electrolyte Fuel Cell Components.

Material	Measured k (W/m · K)
DuPont Nafion membrane (at 30°C)	0.16 ± 0.03
W. L. Gore reinforced electrolyte	0.16 ± 0.03
Toray carbon fibar paper diffusion media (TGP-H at 57°C)	1.76 ± 0.30
SIGRACET 0 wt % PTFE carbon-fiber paper diffusion media (AA series at 56°C)	0.48 ± 0.09
SIGRACET 5 wt % PTFE carbon-fiber paper diffusion media (BA series at 58°C)	0.31 ± 0.06
SIGRACET 20 wt % PTFE carbon-fiber paper diffusion media (DA series 58°C)	0.22 ± 0.04
E-Tek ELAT carbon cloth diffusion media (LT1200-W at 33°C)	$0.22^a \pm 0.04$
Catalyst layer (0.5 mg/cm^2 platinum on carbon)	$0.27^a \pm 0.05$

[a]Effective thermal conductivity (includes thermal contact resistance with diffusion media)
Source: From [49].

Table 5.15 Thermal Conductivity of Fuel Cell Components

Material	Thermal Conductivity (W/m · K) @25 °C
Platinum	70
Nickel	91
7% YSZ (SOFC electrolyte)	~2.0 [56]
Pure Graphite	~90
Stainless steel	16
Aluminum Oxide	30
Aluminum	250
Carbon	1.7
Steel	46
Teflon™	0.25
Fiberglass	0.04
Oxygen	0.024
Nitrogen	0.024
Hydrogen	0.17
Water vapor	0.016
Liquid water	0.58
Methanol	0.21

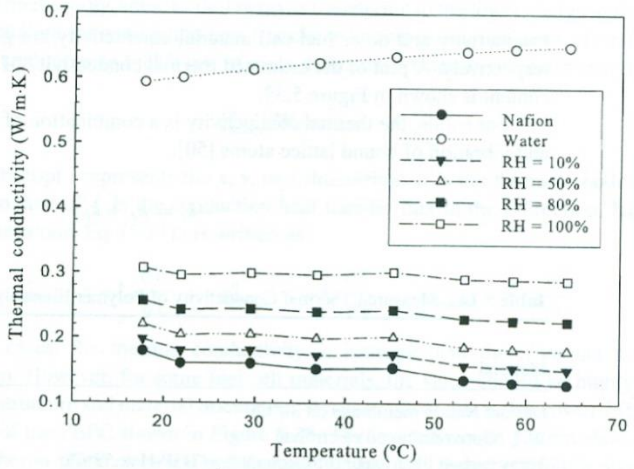

Figure 5.39 Estimated thermal conductivity of Nafion 1100 EW at different humidity ratios. The thermal conductivity variation of pure water is shown as an upper bound for the theoretical moist Nafion thermal conductivity [49].

-For solid, thermal conductivity is a combination of a transport of free electrons and vibration of bound lattice atoms

$$k_t = k_e + k_l$$

-for electrical conductors such as metals, electronic conductivity portion dominates.

Thermal and electrical resistances can be correlated by the Wiedemann-Franz law

-for electrical insulators (such as electrolyte), lattice vibration thermal conductivity dominates.

The more ordered and crystalline the structure is, the greater the thermal conductivity

For gases, thermal conductivity increases with temp

→ for fuel cell, thermal conductivity of H_2 is 5~10 times greater than for air or water vapor → greater fraction of heat is transported through anode than through cathode flow

- **Convection: internal correlations and definitions**

-mass and heat transport in fuel cells is not only by diffusion and conduction → convection is important

-convection: a result of the motion of the fluid field

(i) Forced convection: fluid motion that is a result of forced input, such as a fan or pump

(ii) Natural convection: a result of density gradient in the flow which cause motion

-heat flux from a surface at temp, s, to a fluid at temp, m

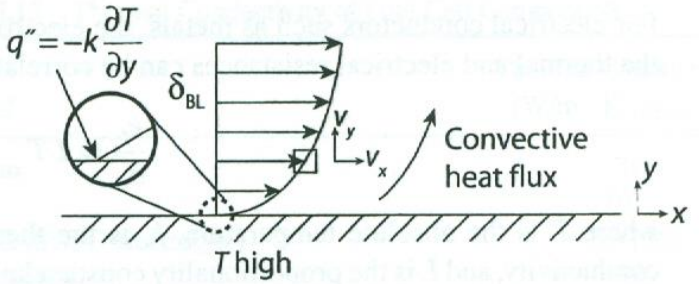

Figure 5.40 Schematic of fluid flowing over heated interface showing local conduction at interface and advection of heat through boundary layer. The sum of the molecular-level interaction conduction and heat transfer by bulk motion (advection) is terms the convection heat transfer.

-Nusselt number: thermal conductivity and length scale of heat transfer to the convection coefficient

Table 5.16 Nusselt Number for Various Rectangular Geometries

Cross Section ($b \times a$)	b/a	Boundary Condition: Uniform Heat Flux, $Nu = hL/k$	Boundary Condition: Uniform Surface Temperature, $Nu = hL/k$
Circular	NA, any diameter	3.11	2.47
Triangular	NA, equilateral triangle	4.36	3.66
Rectangular	1	3.61	2.98
Rectangular	1.43	3.73	3.08
Rectangular	2	4.12	3.39
Rectangular	3	4.79	3.96
Rectangular	4	5.33	4.44
Rectangular	8	6.49	5.6
Rectangular	∞	8.23	7.54

Source: Adapted from [51].

-Thermal entry length for laminar flow

Example 5.17 Estimated Temperature Gradient inside a PEFC

Consider a typical PEFC operating at 0.6 V generating around 0.6 W/cm^2 waste heat flux. Determine the expected temperature gradient from the 400-μm-thick cloth DM to the cathode catalyst layer, assuming 50% of the waste heat is removed from the cathode side.